# Parameterization of Mangrove Root Structure of *Rhizophora stylosa* in Coastal Hydrodynamic Model

Nobuhito Mori[1,2]\*, Che-Wei Chang[1], Tomomi Inoue[3], Yasuaki Akaji[3], Ko Hinokidani[4], Shigeyuki Baba[5], Masashi Takagi[6], Sotaro Mori[6], Hironoshin Koike[6], Miho Miyauchi[6], Ryosuke Suganuma[6], Audrius Sabunas[6], Takuya Miyashita[1] and Tomoya Shimura[1]

[1]Disaster Prevention Research Institute, Kyoto University, Kyoto, Japan, [2]Graduate School of Engineering, Swansea University, Swansea, United Kingdom, [3]National Institute for Environmental Studies, Tsukuba, Japan, [4]Graduate School of Agriculture, Tokyo University of Agriculture, Tokyo, Japan, [5]International Society for Mangrove Ecosystems, Okinawa, Japan, [6]Graduate School of Engineering, Kyoto University, Kyoto, Japan

Mangroves are able to attenuate tsunamis, storm surges, and waves. Their protective function against wave disasters is gaining increasing attention as a typical example of the green infrastructure/Eco-DRR (Ecosystem-based Disaster Risk Reduction) in coastal regions. Hydrodynamic models commonly employed additional friction or a drag forcing term to represent mangrove-induced energy dissipation for simplicity. The well-known Morison-type formula (Morison et al. 1950) has been considered appropriate to model vegetation-induced resistance in which the information of the geometric properties of mangroves, including the root system, is needed. However, idealized vegetation configurations mainly were applied in the existing numerical models, and only a few field observations provided the empirical parameterization of the complex mangrove root structures. In this study, we conducted field surveys on the Iriomote Island of Okinawa, Japan, and Tarawa, Kiribati. We measured the representative parameters for the geometric properties of mangroves, *Rhizophora stylosa,* and their root system. By analyzing the data, significant correlations for hydrodynamic modeling were found among the key parameters such as the trunk diameter at breast height (*DBH*), the tree height *H*, the height of prop roots, and the projected areas of the root system. We also discussed the correlation of these representative factors with the tree age. These empirical relationships are summarized for numerical modeling at the end.

Keywords: mangrove, prop roots, *Rhizophora stylosa*, root structure, parameterization

## INTRODUCTION

Green infrastructure, known as ecosystem-based disaster risk reduction (Eco-DRR), has become popular in the context of coastal flooding reduction following the *Intergovernmental Panel on Climate Change Fifth Assessment Report*, AR5 (Intergovernmental Panel on Climate Change (IPCC) Fifth Assessment Report—Working Group II, 2014) and the *Sendai Framework for Disaster Risk Reduction* 2015–2030 (UNISDR,2015). Its cost-efficiency, capability, and sustainability of adapting to changing climate have been drawing attention worldwide (e.g., Sutton-Grier et al., 2015; Guannel et al., 2016; Reguero et al., 2018).

As natural barriers against coastal hazards, green infrastructures primarily regard coastal dunes, sandy beaches, coastal forests, mangroves, coral reefs, and wetlands. Coastal trees and mangroves are recognized for their protective function in terms of the reduction of wave/hydrodynamic energy during extreme events (e.g., storm waves, surges, and tsunamis). Based on several reports of the 2011 Tohoku Earthquake Tsunami (e.g., Tanaka 2012), coastal pines can be critical in attenuating wave energy under small-to medium-sized tsunamis. Another major type of coastal vegetation, mangroves were identified as useful buffers in the tropics and subtropics during the 2004 Indian Ocean Earthquake Tsunami (e.g., Danielsen et al., 2005) and other major natural disasters (e.g., Goda et al., 2019). In addition to their protective function against coastal disasters, afforestation and reforestation of mangroves have been adopted in Southeast Asia and the Pacific islands to improve the capacity for carbon storage and environmental recovery as a measure of climate change mitigation. Despite the findings in simplified analytical and numerical modeling of wave attenuation based on the other vegetation study, the current scientific knowledge and modeling tools to assess the effectiveness of mangroves are relatively limited considering the realistic shape of mangroves (e.g., Chang and Mori 2021). Generally, a forcing term in the Euler equation or shallow-water equation is used to account for the energy dissipation by vegetation in various studies (e.g., Dalrymple et al., 1984; Mendez and Losada 2004; Mazda et al., 2005). The vegetation effects were integrated as enhanced bottom friction in some studies (e.g., Augustin et al., 2009; Yang et al., 2015), while the Morison-type formula (Morison et al., 1950) has recently been considered more straightforward to parameterize vegetation-induced resistance (e.g., Huang et al., 2011; Chakrabarti et al., 2017; Alagan Chella et al., 2020).

Despite the development of numerical models, idealized vegetation conditions (e.g., cylinders) or bottom friction was mostly applied in the models mentioned above, indicating an over-simplification of the structural complexity of mangrove root systems. The complex root system of mangroves reduces flow velocity and dissipate wave energy (e.g., Tanaka et al., 2007; Zhang et al., 2015) and is necessary to be well addressed in numerical modeling. Based on the Morison-type formula, the general expression of vegetation-induced force $\boldsymbol{R}_{vg}$ can be written as a summation of the drag force and the inertia force:

$$\boldsymbol{R}_{vg} = \frac{1}{2(\eta + h)}C_D \int_{-h}^{\eta} \boldsymbol{u}|\boldsymbol{u}|d\boldsymbol{A}(z) + \frac{1}{(\eta + h)}C_M \int_{-h}^{\eta} \frac{\partial \boldsymbol{u}}{\partial t}d\boldsymbol{V}(z) \quad (1)$$

where $\eta$ represents the free surface elevation, $h$ the water depth, $u(z)$ the fluid velocity, and $C_D$ and $C_M$ the drag and inertia coefficients, respectively. The vertical variation of the frontal area and the submerged volume of mangroves are included in $A(z)$ and $V(z)$ of **Eq. 1**. The effects of mangroves can be modeled in terms of $C_D$, $C_M$, $A(z)$, and $V(z)$, which are all related to mangrove structure (morphology). A recent experimental study (Chang et al., 2019) reproduced the root structures of a specific mangrove by using 3D scanned and 3D-printed tree models in laboratory tests. With direct measurements of wave forces exerted on tree models, the empirical formulas to estimate the force coefficients ($C_D$ and $C_M$) were proposed. As indicated in Zhang et al. (2015) and Chang et al. (2019), proper parameterization, including the complex structure of mangrove roots based on field conditions, is needed to quantify better mangrove effects on wave attenuation in the development of numerical models. However, there are very limited mangrove structure data that are related to hydrodynamic models, such as **Eq. 1** and the others.

The *Genus Rhizophora* consists of seven species (Tomlinson 2016) and are widely distributed along tropical and subtropical coastlines (Duke 2006). They are also common species used for mangrove afforestation and reforestation. As *Rhizophora* species have complex bifurcated and looping structures (so-called prop root system), several researchers conducted field surveys on *Rhizophora* species for root structure (e.g., Ohira et al., 2013; Mendez-Alonzo et al., 2015). They examined the parameterization of mangrove root structures (e.g., the relationship between tree height and the trunk diameter at breast height) to understand their shape characteristics. Besides biological interests, parametrization of trunk shape is quite essential for wave attenuation. Ohira et al. (2013) measured the trunk shapes and estimated the hydraulic resistance in tsunami inundation simulations. Based on their proposed relations, the projected area and submerged volume of mangrove roots can be calculated and used in numerical computations. However, their target was large and older trees, and the variation of shape parameters associated with the tree age was not discussed in their study, which is not enough for the model application targeting early to middle term of afforestation and reforestation. The biological and physical characteristics (e.g., Komiyama et al., 2008) in addition to the structural properties, should be well addressed in the future development of numerical models when considering the impact of changing climate under a longer time scale.

In this study, we conducted field surveys to collect the fundamental characteristics of mangrove tree shape by focusing on the *Rhizophora* species. Based on the field data analysis, the relationships among different geometric diameters and the tree age are examined, although the available field data is limited. The parameterization of the shape of *Rhizophora* species is proposed for the future development of coastal wave models. In the following, the outline of the field surveys and the data processing procedures are provided in *Outline of Field Survey and Measurements*. The parameterization of mangrove root structure is presented in *Results and Discussions*. Finally, the results of the current study are summarized in *Summary*.

# OUTLINE OF FIELD SURVEY AND MEASUREMENTS

## Survey Areas

Two sets of field surveys were conducted in 2019 and 2020 to investigate mangrove root structure. The field sites included natural mangrove forests in the Iriomote Island of Okinawa, Japan, and a planted mangrove area in Tarawa, Kiribati.

Iriomote Island, one of the Yaeyama Islands in Okinawa Prefecture, Japan, is a subtropical island located in the Northwest Pacific Ocean, as shown in the upper panel in **Supplementary Figure S1**. As a part of the Ryukyu Islands Archipelago, Iriomote Island is mountainous (highest altitude: 470 m) with 29 rivers culminating in the coast. The island is 290 km² in area, and the majority of its landmass is covered by natural forests, in which 85% is national forests. Mangrove forests are mainly located in the low-lying areas along the rivers with several species such as *Rhizophora stylosa* Griff. and *Bruguiera gymnorhiza* L. (Lam.) targeting one of the dominant species distributed in estuaries and tidal areas, *R. stylosa,* we conducted surveys on natural mangroves along the Urauchi River (the longest river in Iriomote), as shown in the **Supplementary Figure S1**. Natural mangroves in an estuary were selected for the measurements. The effect of waves is very limited in this area. Several isolated mangroves were picked for field measurements due to the difficulty of imaging measurements.

The other field site was Tarawa, Kiribati, a tropical island located in the Central Pacific Ocean (1°27′ N, 172°58′ E), as shown in the **Supplementary Figure S1**. Tarawa is an atoll comprising a long flat reef partially enclosing a shallow lagoon with a wide range of astronomical tides. It is 500 km² in area, and the highest altitude is 3 m. *R. stylosa* has been planted by the International Society for Mangrove Ecosystems (ISME) since 2005 for multiple purposes, such as environmental recovery, coastal protection, and environmental education. Each year around 7,000–11,000 propagules were planted uniformly with 50 cm as the tree spacing by the close group planting method (Baba, 2011) in the designated afforested patches. The afforestation areas are mainly located west of Bonriki in Tarawa with calm coastal environmental conditions to avoid exposure to severe wind waves and swells. The effect of waves is very limited due to geophysical effects in this area. Therefore, the afforested mangroves inside of the atoll were selected for the measurements. Thus, clear records can be obtained, including the date of afforestati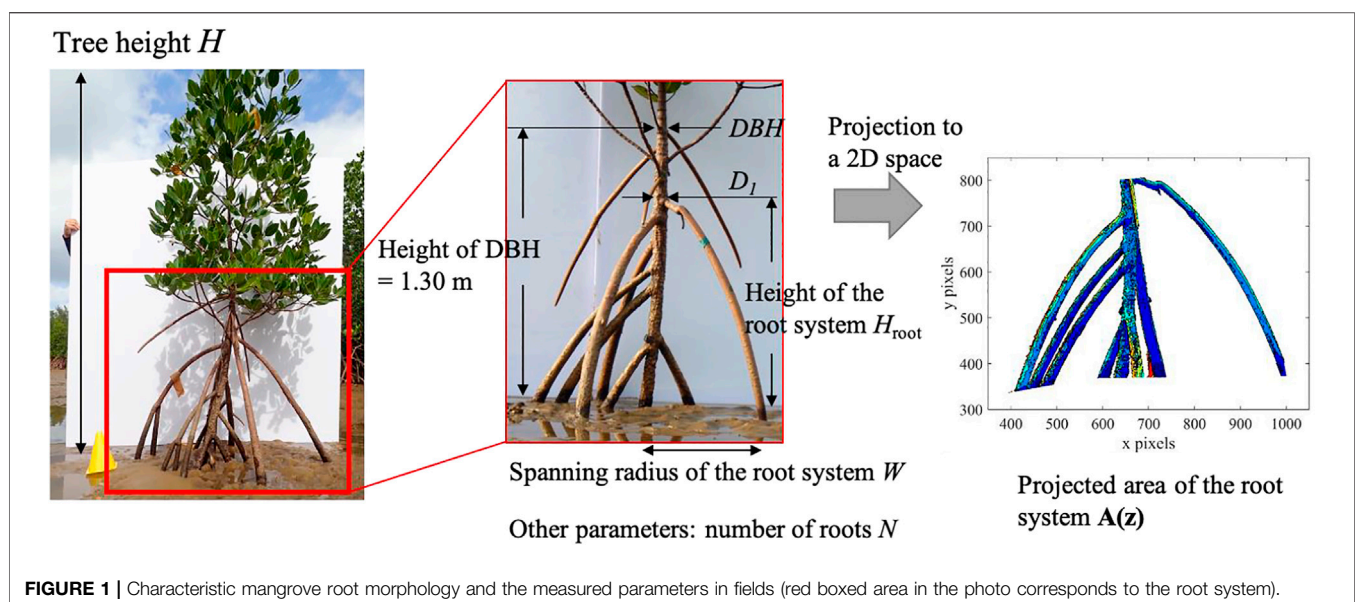on, density, and others in this area. Comparing with natural forests, the afforested mangroves in Tarawa provided an ideal condition to investigate the relationship between mangrove root structure and the associated tree age (**Supplementary Figure S2**).
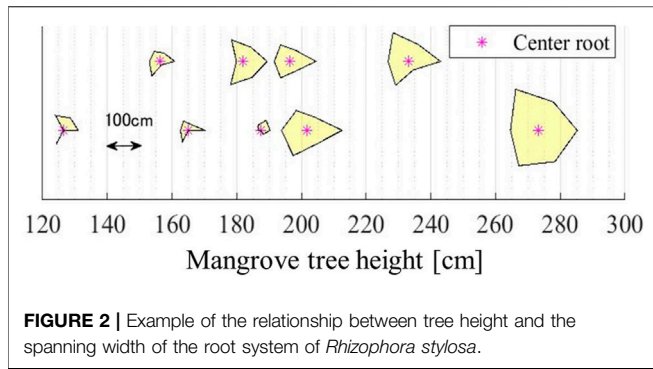
In both surveys, the fieldwork included the manual measurements of the representative parameters of mangrove root structure and the use of a 3D laser scanner for detailed root structures. In addition, the 2D projected visualization of mangrove root shapes was obtained by using a digital camera in Iriomote Island. As the 2D and 3D visualization measurements required space, we selected front trees of groups, but the basic tree characteristics (e.g., tree heights, DBH, or age) were measured both front and inside of trees in Tarawa. In this paper, we analyzed the field measurements and the 2D image visualization of mangrove root system structure. At the same time, the 3D scanned data will be presented in the forthcoming analysis along with further field surveys in future work.

## Methodology

Firstly, we measured the characteristic geometry of mangrove structure, *R. stylosa*, in fields. As shown in **Figure 1**, the measured parameters included the tree height $H$ and the trunk diameter at breast height ($DBH$), which refers to the measured diameter at 1.30 m above the ground. We also measured the trunk diameter at the top of the root system $D_1$ (equivalent to $DBH$ for a shorter tree), the height of the root system $H_{root}$, and the spanning radius of the root system $W$ (i.e., the distance from the tree trunk to the outermost root). Note that the spanning radius was measured in six major orientations whose average was used as characteristic $W$. The six orientations of spanning radius were combined major two axes plus four major roots. Furthermore, avoiding the difficulty of measurement, the diameter of individual roots was measured at 20 cm above the ground, and the number of prop roots $N$ was recorded. Forty-two trees were picked for field measurements in Iriomote Island and four trees in Tarawa, Kiribati.

In addition to the measurements of the representative parameters of mangrove root structure, we collected the 2D



**FIGURE 1 |** Characteristic mangrove root morphology and the measured parameters in fields (red boxed area in the photo corresponds to the root system).

**FIGURE 2 |** Example of the relationship between tree height and the spanning width of the root system of *Rhizophora stylosa*.
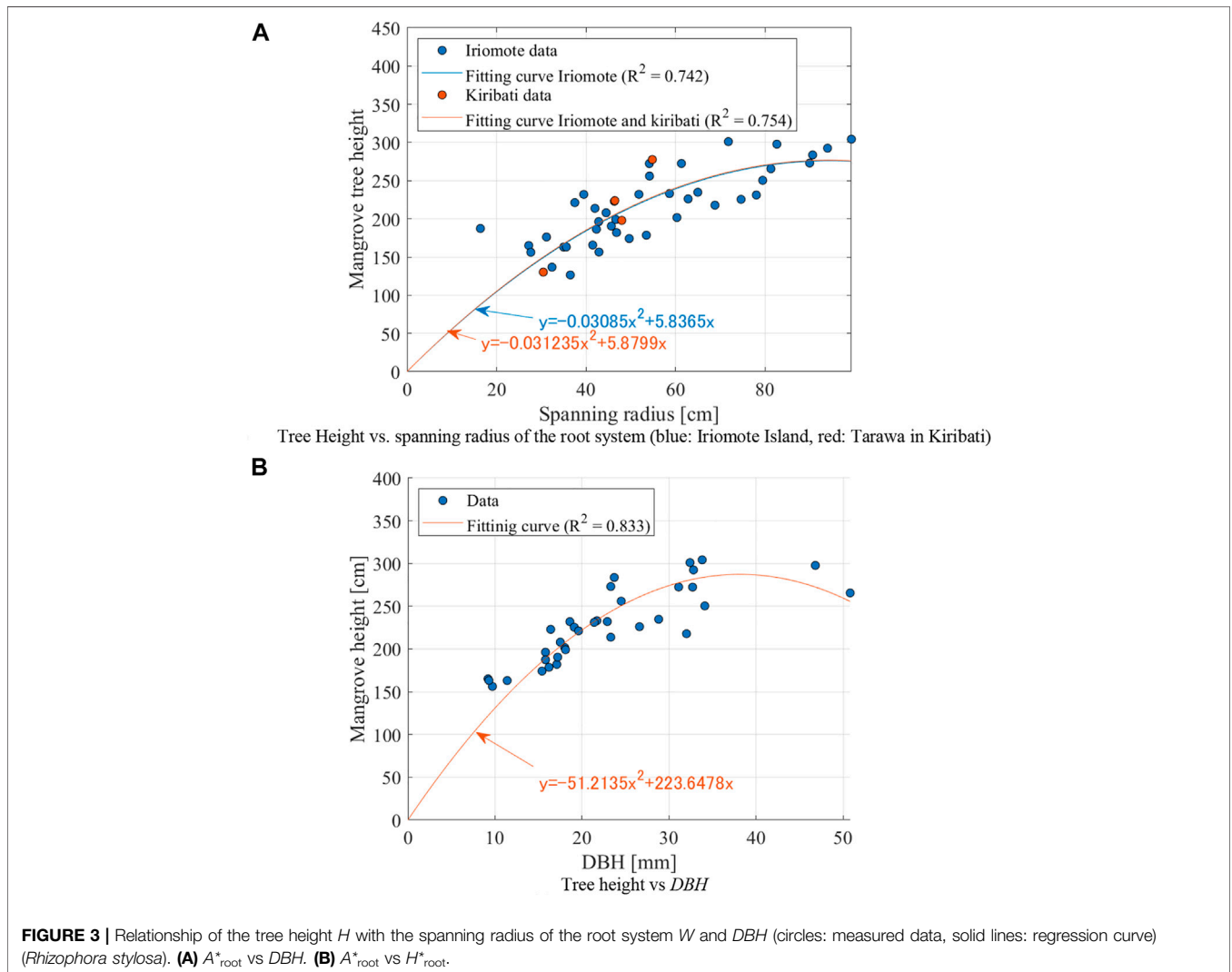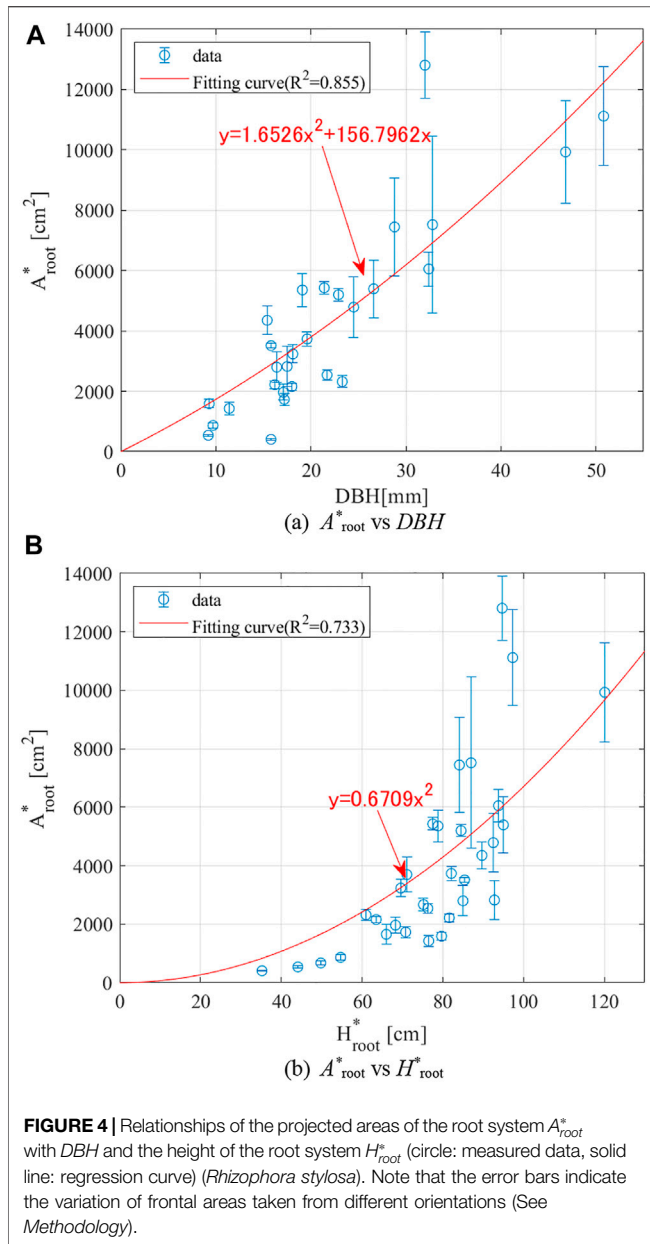
Following the previous studies (salt marsh by Lemein et al., 2015, mangrove by Maza et al., 2017), the projected area of the root system $A_{root}$ can then be estimated by image processing as shown in **Supplementary Figure S2**. We summarize the procedures for image processing as follows.

1. Binarize the image using the threshold values of the RGB image.
2. Extract the outline of the root system from the binary image (left panel in **Supplementary Figure S3**).
3. Extract the root system from the RGB image in step 2 (right panel in **Supplementary Figure S3**).
4. Counting the number of pixels of the root system in step 3.
5. Convert pixel to length scale.

Note that step 2 focuses on the image analysis, excluding the outside area of the root system. Image preprocessing in steps 1 and 2 can reduce the misperception of the analysis. In some cases, sunlight may disturb the color intensity of the image; therefore, the effect was corrected in steps 2 and 3 manually. The counted

images of mangrove roots using a digital camera (Olympus TG-6, 4,000 × 3,000 pixels) along with a whiteboard as the background (**Figure 1**). The 2D images were taken in two different directions in two major axes of the root system, and no image correction was applied due to the difficulty of the detail of calibration in the field.



**FIGURE 3 |** Relationship of the tree height *H* with the spanning radius of the root system *W* and *DBH* (circles: measured data, solid lines: regression curve) (*Rhizophora stylosa*). **(A)** $A^*_{root}$ vs *DBH*. **(B)** $A^*_{root}$ vs $H^*_{root}$.

FIGURE 4 | Relationships of the projected areas of the root system $A^*_{root}$ with *DBH* and the height of the root system $H^*_{root}$ (circle: measured data, solid line: regression curve) (*Rhizophora stylosa*). Note that the error bars indicate the variation of frontal areas taken from different orientations (See *Methodology*).



FIGURE 5 | Relationship between the normalized projected area of the root system $A_{root}$ and the normalized distance *z* from the ground (circle: measured data, solid line: regression curve) (*Rhizophora stylosa*).

number of pixels was in the range 10,000–242,000, which is equivalent to approximately 300–3,700 cm$^2$. As the number of pixels was sufficient to capture the area of the root system, the accuracy of the estimated projected area was reliable for further discussions with other parameters.

## RESULTS AND DISCUSSIONS

### Relationships Among the Main Parameters of Mangrove Root Structure

We first examined the measured tree height and the main geometric parameters of the root system. Major three axes were analyzed by the 2D imaging following *Methodology*. In
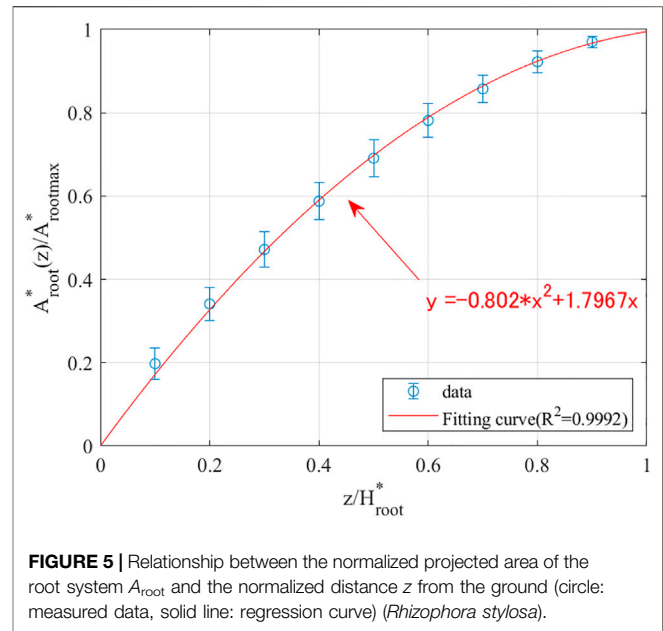
**Figure 2**, a proportional relationship can be seen between the tree height *H* and the spanning radius of the root system *W*. Asymmetric root system can also be observed for shorter trees (approximately <180 cm). These morphological characteristics of mangrove trees and root systems are discussed in this section. As the spanning radius of the root system varied in different orientations, the averaged value was applied hereafter.

**Figure 3A** shows the relationship between the tree height *H* and the spanning radius *W* by Iriomote Island and Tarawa with two empirical fitting formulas presented by blue and red solid lines, respectively. Note that zero intercepts were assumed when defining the empirical fitting formula. Obviously, these two parameters are highly correlated, as presented in **Figure 2**. Although the data in Tarawa is fewer than Iriomote Island, two different data in different locations show the quite similar relation for *H* and *W*. Next, the relationship between the tree height *H* and the trunk diameter at breast height *DBH* for Iriomote Island data with the empirical fitting formula is shown in **Figure 3B**. According to the measurements, the tree height increases linearly with smaller *DBH* (<25 mm) and tends to be convergent around 300 cm for larger *DBH* (>30 mm) within the measured *DBH* range (<50 mm). Note that the comparison with the results in Ohira et al., 2013 for *Rhizophora apiculata* Blume and *Rhizophora mucronata* Lam. with this dataset is quite similar but slightly higher tree height by the current parameterization for *R. stylosa*.

Secondly, we discussed some of the representative parameters of the root system. **Supplementary Figure S4** shows the proportional relationship between the height of the root system $H_{root}$ and the number of prop roots *N*, which can be expected as a part of the natural growing process. Note that the height of the root system was estimated by analyzing the 2D images taken from different orientations (*Methodology*), and an averaged value (with an asterisk) is presented here. The results
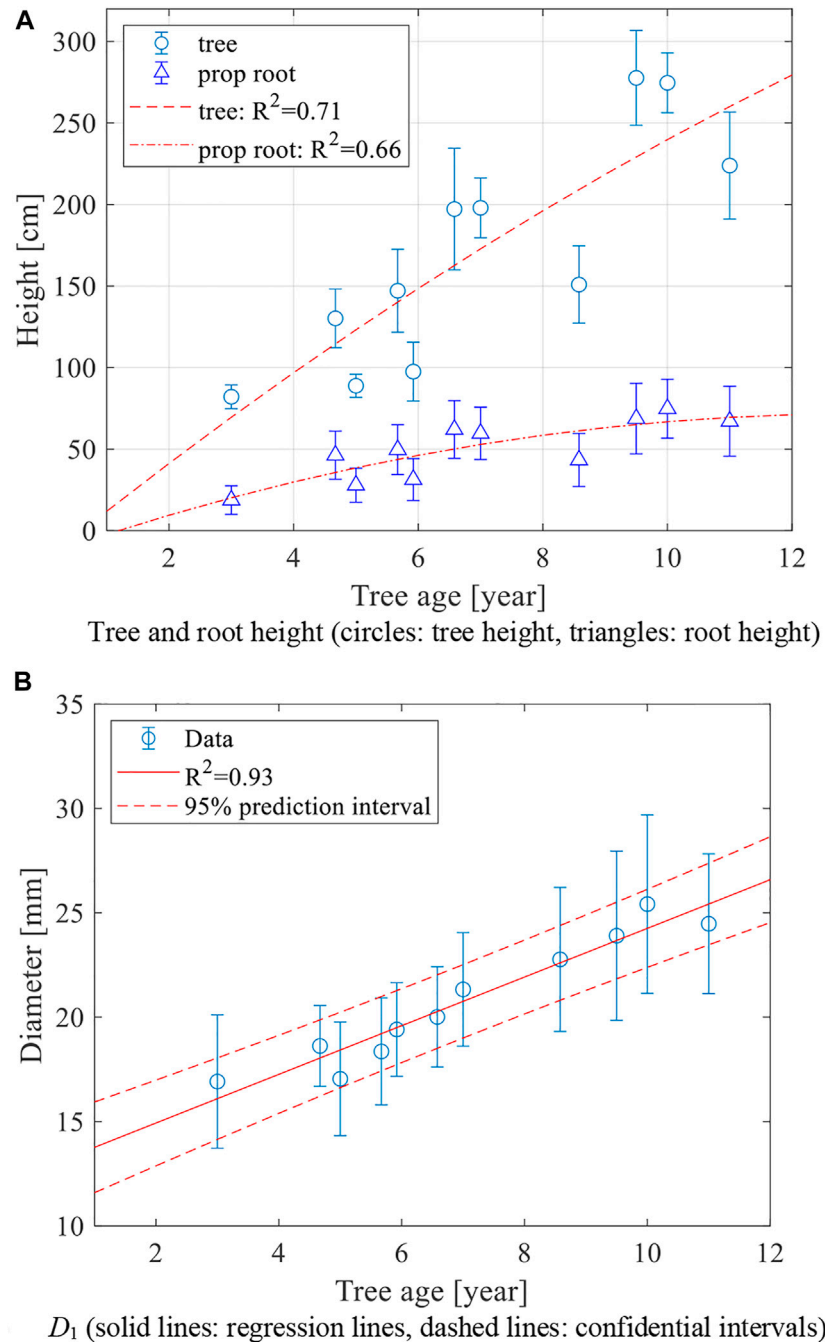
**FIGURE 6 |** Growth curves of diameter $D_1$ and tree height $H$ vs. tree age by Kiribati data (*Rhizophora stylosa*).

reported in Ohira et al., 2013 were also included in the same figure for comparison, although their target mangrove species are *R. apiculata* and *R. mucronata.*

In addition to the relationships among distinguishing factors of mangrove root structure, another objective of this study was to understand the intertwined connections between the aforementioned geometric parameters and the projected area of the root system, which is critical to establish the proper parameterization of mangrove effects as shown in **Eq. 1**.

Therefore, we here present the projected area of the root system $A_{root}^*$ and its relationships with two representative parameters of mangrove root structure—*DBH*, and $H_{root}^*$. In **Figure 4A**, the projected area $A_{root}^*$ increases with *DBH*, in which *DBH* approximately ranges from 8 to 52 mm, monotonically. The projected area $A_{root}^*$ against the height of the root system $H_{root}^*$ can be found in **Figure 4B**, showing a quadratic proportional relationship. Both the relation of *DBH* and $H_{root}^*$ to $A_{root}^*$ shows quadric increases as their increase. It indicates the nonlinear increase
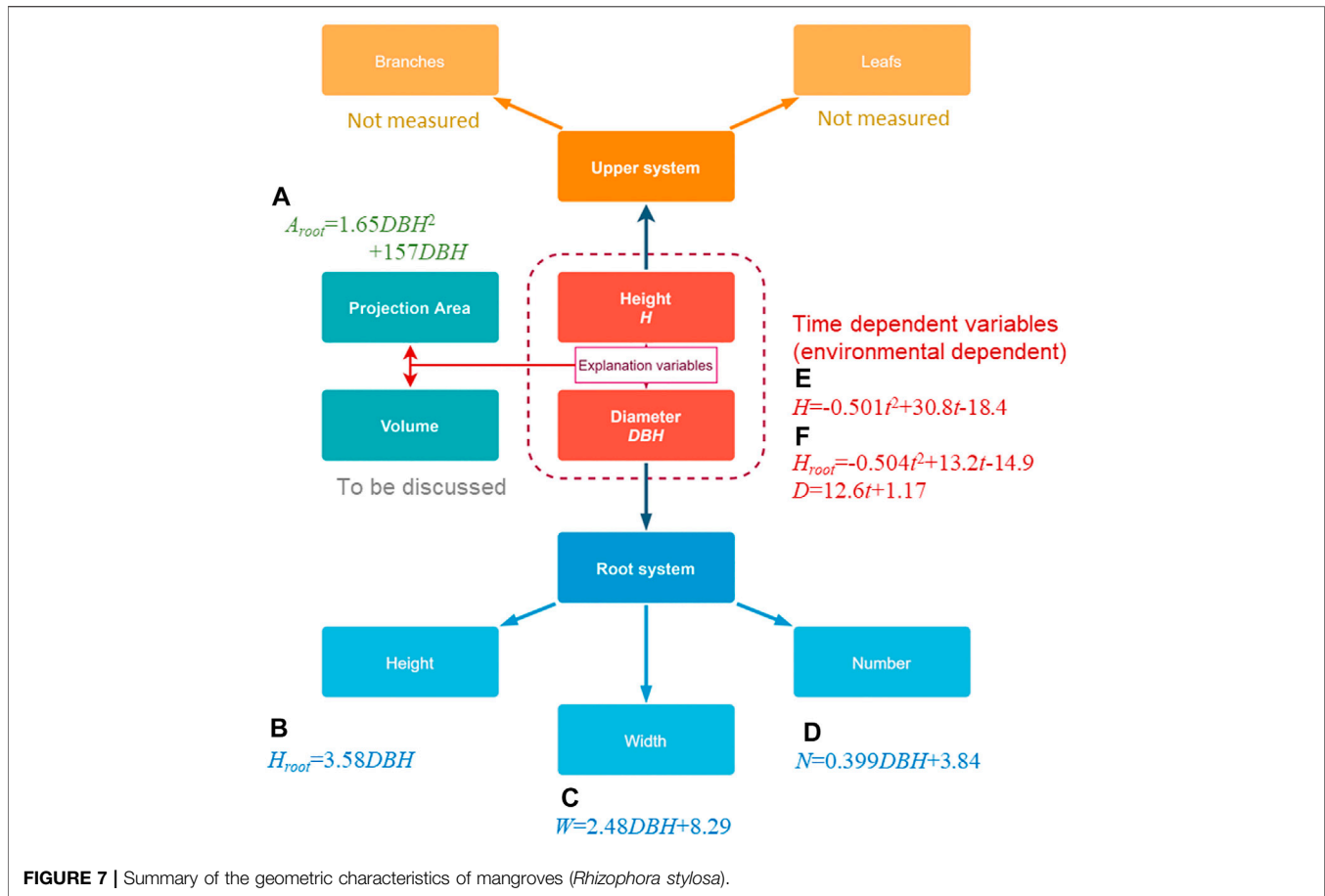
**FIGURE 7 |** Summary of the geometric characteristics of mangroves (*Rhizophora stylosa*).

of wave damping by the root system as the mangrove becomes larger. Furthermore, **Figure 5** shows the normalized $A_{root}^*$ in terms of the normalized vertical distance $z$ from the bottom by $H_{root}^*$. Both the ensemble average and its standard deviation are presented. The normalized frontal area quadratically increases from the bottom, and it gradually approaches the maximum near the top of the root system. As observed in fields, the projected area of mangrove roots shows nonlinear profiles (unlike other coastal trees with relatively simple geometry), which need to be properly parameterized, especially under low water-level conditions.

The current analysis obtained the empirical relationships among the representative parameters of mangrove root structure and the root system. Although solely using the relationship based on *DBH* in numerical modeling may yield uncertainties by ignoring the contributions from other factors, the above results relate other characteristics of mangrove root structure (e.g., height of the root system, the number of prop roots and the frontal area of the root system) which shall compensate the parameterization in numerical modeling.

## Relationships Between Tree Age and Geometric Characteristics

As presented in the previous section, the bulk geometric characteristics of mangroves and the root system can be parameterized as a function of tree height $H$, *DBH*, and height of prop roots $H_{root}$. On the other hand, the information on these parameters and their variation in time is critical to assess mangrove effects on wave damping, especially when conducting afforestation or reforestation. The potential impact of growth rate on mangrove root structure should also be included in the development of numerical models for longer time-scale estimation (e.g., in 10 years or later).

In **Figure 6A**, we first present the relationships of tree age with the tree height (circles) and the height of the prop roots (triangles) by Kiribati data. The regression curves (dashed lines) obtained by the least-square fitting method are included in the same plot. A higher growth rate of the tree height was observed in comparison with that of the root system. Recalling the quasi-linear relationship between $H$ and $W$ in **Figure 3A**, the increasing rate of the spanning radius of the root system (as well as the number of prop roots) can be expected to be greater compared to the growth rate of the height of mangrove roots. It should also be noted that the growth or height of the root system is not only determined by age but also the other environmental conditions. Therefore, the shown relation in **Figure 6** is neither directly related to Iriomote Island data or general. The field variation and the different site-to-site environmental conditions should be considered when discussing the proper parameterization quantitatively. However, the summary of the combined field

data can give us the first approximation of mangrove shape parameterization for hydrodynamic modeling.

In **Figure 6B**, the diameter $D_1$ is plotted versus the tree age. Note again that $D_1$ denotes the trunk diameter right above the root system. A clear linear relationship can be observed in **Figure 6B**, and the regression curve is also provided. The diameter $D_1$ approximately ranges from 15 mm (3-year-old tree) to 25 mm (11-year-old tree). The empirical relationships in **Figures 6A,B** provide a valuable reference to estimate the variation of the representative parameters of mangrove root structure in time.

## SUMMARY

In this study, we conducted two field surveys in the Iriomote Island of Okinawa, Japan, and Tarawa, Kiribati. Targeting at the parameterization of mangrove root structure, we collected the representative characteristics of mangrove geometry in fields, such as the tree height, the height of the root system, the spanning width of mangrove roots, the trunk diameter, and the frontal projected area. By analyzing the field data, we aimed to find out empirical formulas among the characteristic parameters of mangrove root geometry which are critical for the implementation of mangrove effects in numerical models for wave propagation.

Distinct relationships were found among the tree height, the spanning radius, the trunk diameter at breast height (*DBH*), and the projected area $A(z)$ of the root system. Here, we summarize the estimated relationships of mangrove bulk characteristics in **Figure 7** (see additional data in **Supplementary Figures**). Based on **Figure 7**, we can estimate the root height, root width, and the number of the root system as well as the frontal projected area A(z) as a function of tree age *t*. Although the upper system of the mangrove (i.e., leaves and branches) was not measured, we succeeded in obtaining several empirical relationships in terms of the representative factors of mangrove geometry as an example. As presented in **Eq. 1**, one of the key factors to determine mangrove effects in wave modeling is the frontal projected area $A(z)$ of the root system. Applying the empirical relationships along with the Morison-type formula in **Eq. 1**, mangrove-induced dissipation can be parameterized in numerical models with inputs of field measurements of the characteristic geometric diameters and heights. To account for the potential impacts of the growth rate of mangroves, we also analyzed the relationship of the tree age with the tree height and

the trunk diameter $D_1$ (or DBH). Both the tree heights and trunk diameter showed monotonically increasing relationships with the tree age. This information is useful in future long-term assessment of mangrove effects, especially in the afforested or reforested areas.

It is necessary to continue field surveys in different environments and accumulate the dataset to cover other parameters, parameter spaces and reduce the uncertainty for parameterizing mangrove effects in numerical modeling. The detailed 3D structures and shapes of mangrove roots will be discussed using the 3D scanned data. More measurements such as the upper system (e.g., leaves and branches), other physical properties of mangroves (e.g., stiffness) and density of trees will be included in the next phase of the field survey.

## DATA AVAILABILITY STATEMENT

The raw data supporting the conclusion of this article will be made available by the authors, without undue reservation.

## AUTHOR CONTRIBUTIONS

NM, C-WC led the research and wrote the main part of the manuscript. TI, YA, KH, SB, AS, TM, and TS conducted a field survey and analyzed data in Kiribati. MT, SM, HK, MM, and RS conducted a field survey and analyzed data in Iriomote.

## FUNDING

## SUPPLEMENTARY MATERIAL

The Supplementary Material for this article can be found online at: https://www.frontiersin.org/articles/10.3389/fbuil.2021.782219/full#supplementary-material

## REFERENCES

Alagan Chella, M., Kennedy, A. B., and Westerink, J. J. (2020). Wave Runup Loading Behind a Semipermeable Obstacle. *J. Waterway, Port, Coastal, Ocean Eng.* 146, 04020014. doi:10.1061/(asce)ww.1943-5460.0000569

Augustin, L. N., Irish, J. L., and Lynett, P. (2009). Laboratory and Numerical Studies of Wave Damping by Emergent and Near-Emergent Wetland Vegetation. *Coastal Eng.* 56, 332–340. doi:10.1016/j.coastaleng.2008.09.004

Baba, S. (2011). Close Group Planting of Mangroves on Atolls and Coral Islands of the Pacific. *ISME/GLOMIS Electron. J.* 9 (4), 11–12.

Chakrabarti, A., Brandt, S. R., Chen, Q., and Shi, F. (2017). Boussinesq Modeling of Wave-induced Hydrodynamics in Coastal Wetlands. *J. Geophys. Res. Oceans* 122, 3861–3883. doi:10.1002/2016jc012093

Chang, C. W., and Mori, N. (2021). Green Infrastructure for the Reduction of Coastal Disasters: a Review of the Protective Role of Coastal Forests against Tsunami, Storm Surge, and Wind wavesCoastal Engineering Journal. *Taylor Francis* 63 (3)), 370–385. doi:10.1080/21664250.2021.1929742

Chang, C.-W., Mori, N., Tsuruta, N., and Suzuki, K. (2019). Estimation of Wave Force Coefficients on Mangrove Models. *J. Jpn. Soc. Civil Eng. Ser. B2 (Coastal Eng.)* 75, I_1105–I_1110. doi:10.2208/kaigan.75.i_1105

Dalrymple, R. A., Kirby, J. T., and Hwang, P. A. (1984). Wave Diffraction Due to Areas of Energy Dissipation. *J. Waterway, Port, Coastal, Ocean Eng.* 110, 67–79. doi:10.1061/(asce)0733-950x(1984)110:1(67)

Danielsen, F., Sørensen, M. K., Olwig, M. F., Selvam, V., Parish, F., Burgess, N. D., et al. (2005). The Asian Tsunami: A Protective Role for Coastal Vegetation. *Science* 310, 643. doi:10.1126/science.1118387

Duke, N. C. (2006). *Australia's Mangroves. The Authoritative Guide to Australia's Mangrove Plants.* Brisbane, Australia: University of Queensland, 200p.

Goda, K., Mori, N., Yasuda, T., Prasetyo, A., Muhammad, A., and Tsujio, D. (2019). Cascading Geological Hazards and Risks of the 2018 Sulawesi Indonesia Earthquake and Sensitivity Analysis of Tsunami Inundation Simulations. *Front. Earth Sci.* 7, 261. doi:10.3389/feart.2019.00261

Guannel, G., Arkema, K., Ruggiero, P., and Verutes, G. (2016). The Power of Three: Coral Reefs, Seagrasses and Mangroves Protect Coastal Regions and Increase Their Resilience. *Plos One* 11, e0158094–22. doi:10.1371/journal.pone.0158094

Huang, Z., Yao, Y., Sim, S. Y., and Yao, Y. (2011). Interaction of Solitary Waves with Emergent, Rigid Vegetation. *Ocean Eng.* 38, 1080–1088. doi:10.1016/j.oceaneng.2011.03.003

Intergovernmental Panel on Climate Change (IPCC) Fifth Assessment Report – Working Group II (2014). *Climate Change 2014: Impacts, Adaptation, and Vulnerability.* New York, NY: Cambridge University Press.

Komiyama, A., Ong, J. E., and Poungparn, S. (2008). Allometry, Biomass, and Productivity of Mangrove Forests: A Review. *Aquat. Bot.* 89, 128–137. doi:10.1016/j.aquabot.2007.12.006

Lemein, T., Cox, D., Albert, D., and Mori, N. (2015). Accuracy of Optical Image Analysis Compared to Conventional Vegetation Measurements for Estimating Morphological Features of Emergent Vegetation. *Estuarine, Coastal Shelf Sci.* 155, 66–74. doi:10.1016/j.ecss.2014.12.051

Maza, M., Adler, K., Ramos, D., Garcia, A. M., and Nepf, H. (2017). Velocity and Drag Evolution from the Leading Edge of a Model Mangrove forest. *J. Geophys. Res. Oceans* 122 (11), 9144–9159. doi:10.1002/2017jc012945

Mazda, Y., Kobashi, D., and Okada, S. (2005). Tidal-scale Hydrodynamics within Mangrove Swamps. *Wetlands Ecol. Manage.* 13, 647–655. doi:10.1007/s11273-005-0613-4

Méndez-Alonzo, R., Moctezuma, C., Ordoñez, V. R., Angeles, G., Martínez, A. J., and López-Portillo, J. (2015). Root Biomechanics in Rhizophora Mangle: Anatomy, Morphology and Ecology of Mangrove's Flying Buttresses. *Ann. Bot.* 115 (5), 833–840. doi:10.1093/aob/mcv002

Mendez, F. J., and Losada, I. J. (2004). An Empirical Model to Estimate the Propagation of Random Breaking and Nonbreaking Waves over Vegetation fields. *Coastal Eng.* 51, 103–118. doi:10.1016/j.coastaleng.2003.11.003

Morison, J. R., Johnson, J. W., Schaaf, S. A., and Schaaf, S. A. (1950). The Force Exerted by Surface Waves on Piles. *J. Pet. Tech.* 2, 149–154. doi:10.2118/950149-g

Ohira, W., Honda, K., Nagai, M., and Ratanasuwan, A. (2013). Mangrove Stilt Root Morphology Modeling for Estimating Hydraulic Drag in Tsunami Inundation Simulation. *Trees* 27, 141–148. doi:10.1007/s00468-012-0782-8

Reguero, B. G., Beck, M. W., Bresch, D. N., Calil, J., and Meliane, I. (2018). Comparing the Cost Effectiveness of Nature-Based and Coastal Adaptation: A Case Study from the Gulf Coast of the United States. *PLOS One* 13, e0192132–24. doi:10.1371/journal.pone.0192132

Sutton-Grier, A. E., Wowk, K., and Bamford, H. (2015). Future of Our Coasts: The Potential for Natural and Hybrid Infrastructure to Enhance the Resilience of Our Coastal Communities, Economies and Ecosystems. *Environ. Sci. Pol.* 51, 137–148. doi:10.1016/j.envsci.2015.04.006

Tanaka, N., Sasaki, Y., Mowjood, M. I. M., Jinadasa, K. B. S. N., and Homchuen, S. (2007). Coastal Vegetation Structures and Their Functions in Tsunami protection: Experience of the Recent Indian Ocean Tsunami. *Landscape Ecol. Eng.* 3, 33–45. doi:10.1007/s11355-006-0013-9

Tanaka, N. (2012). Effectiveness and Limitations of Coastal forest in Large Tsunami: Conditions of Japanese pine Trees on Coastal Sand Dunes in Tsunami Caused by Great East Japan Earthquake. *J. Jpn. Soc. Civil Eng. Ser. B1* 68, II_7–II_15. doi:10.2208/jscejhe.68.ii_7

Tomlinson, P. B. (2016). *The Botany of Mangroves* (2nd ed.). New York, USA: Cambridge University Press, 418p.

UNISDR (United Nations International Strategy for Disaster Reduction) (2015). *Sendai Framework for Disaster Risk Reduction 2015-2030.* Sendai, Japan: United Nations Office for Disaster Risk Reduction (UNISDR).

Yang, Y., Irish, J. L., and Socolofsky, S. A. (2015). Numerical Investigation of Wave-Induced Flow in mound-channel Wetland Systems. *Coastal Eng.* 102, 1–12. doi:10.1016/j.coastaleng.2015.05.002

Zhang, X., Chua, V. P., and Cheong, H.-F. (2015). Hydrodynamics in Mangrove Prop Roots and Their Physical Properties. *J. Hydro-Environ. Res.* 9 (2), 281–294. doi:10.1016/j.jher.2014.07.010

**Conflict of Interest:** The authors declare that the research was conducted in the absence of any commercial or financial relationships that could be construed as a potential conflict of interest.

**Publisher's Note:** All claims expressed in this article are solely those of the authors and do not necessarily represent those of their affiliated organizations, or those of the publisher, the editors and the reviewers. Any product that may be evaluated in this article, or claim that may be made by its manufacturer, is not guaranteed or endorsed by the publisher.